Eur. Phys. J. A **9**, 277–285 (2000)

THE EUROPEAN PHYSICAL JOURNAL A

Production of a_0-mesons in the reactions $\pi N \to a_0 N$ and $pp \to d a_0^+$ at GeV energies

V.Yu. Grishina[1], L.A. Kondratyuk[2], E.L. Bratkovskaya[3,a], M. Büscher[4], and W. Cassing[3]

[1] Institute for Nuclear Research, 60th October Anniversary Prospect 7A, 117312 Moscow, Russia
[2] Institute of Theoretical and Experimental Physics, B.Cheremushkinskaya 25, 117259 Moscow, Russia
[3] Institut für Theoretische Physik, Universität Giessen, D-35392 Giessen, Germany
[4] Institut für Kernphysik, Forschungszentrum Jülich, D-52425 Jülich, Germany

Received: 4 August 2000
Communicated by W. Weise

Abstract. We investigate the reactions $\pi N \to a_0 N$ and $pp \to d a_0^+$ near threshold and at medium energies. An effective Lagragian approach and the Regge pole model are applied to analyze different contributions to the cross-section of the reaction $\pi N \to a_0 N$. These results are used to calculate the differential and total cross-sections of the reaction $pp \to d a_0^+$ within the framework of the two-step model in which two nucleons produce an a_0-meson via π-meson exchange and fuse to a deuteron. The necessity of new measurements on a_0 production and branching fractions (of its decay to the $K\bar{K}$ and $\pi\eta$ channels) is emphasized for clarifying the a_0 structure. Detailed predictions for the reaction $pp \to d a_0^+$ are presented for the energy regime of the proton synchrotron COSY-Jülich.

PACS. 25.10.+s Nuclear reactions involving few-nucleon systems – 13.75.-n Hadron induced reactions – 13.60.Le Meson production

1 Introduction

The scalar mesons play a very important role in the physics of hadrons since they carry the quantum numbers of the vacuum. Nevertheless, the structure of the lightest scalar mesons $a_0(980)$ and $f_0(980)$ is not yet understood and an important topic of hadronic physics (see, *e.g.*, [1–7] and references therein). It has been discussed that they could be either "Unitarized $q\bar{q}$ states", "Four-quark cryptoexotic states", $K\bar{K}$ molecules or vacuum scalars (Gribov's minions) (see, *e.g.*, ref. [5]). Nowadays, theory gives some preference to the unitarized quark model proposed by Törnqvist [8] (cf. [5,6]). However, other options cannot be ruled out so far. Since there is a strong mixing between the uncharged $a_0(980)$ and the $f_0(980)$ due to a coupling to $K\bar{K}$ intermediate states [3,9], it is important to study independently the uncharged and charged components of the $a_0(980)$ because the latter ones do not mix with the $f_0(980)$ and preserve their original quark content. It is generally expected, furthermore, that the different $a_0(980)$ production cross-sections in πN and NN reactions will provide valuable information on its internal structure.

Until now the charged components of the $a_0(980)$ have been studied dominantly in the $\eta\pi^+$ or $\eta\pi^-$ decay channels [10]. Recent experimental data from the E852 Collaboration at BNL give for the charged a_0^+-meson a mass of 0.9983 ± 0.0040 GeV/c^2 and a width of 0.072 ± 0.0010 GeV/c^2 [11]. Note, that the mass of the a_0 reported by the E852 Collaboration is significantly larger than the average value of 0.9834 ± 0.0009 GeV/c^2 presented in the last issue of the PDG [10].

The branching ratios to the two main a_0 decay channels ($\eta\pi$ and $K\bar{K}$) are still unclear: the $\eta\pi$ mode is quoted by the PDG [10] as "dominant" and the $K\bar{K}$ mode as "seen". We point out, that the data from only two experiments [12,13], where the decay of the $a_0(980)$ to $K\bar{K}$ was observed, have been used for the PDG analysis [10]. The authors of ref. [13] report a ratio of branching ratios

$$\mathrm{Br}(\bar{p}p \to a_0\pi; a_0 \to K\bar{K})/\mathrm{Br}(\bar{p}p \to a_0\pi; a_0 \to \pi\eta) = 0.23 \pm 0.05. \quad (1)$$

However, the second branching ratio taken from ref. [14] might have a systematic uncertainty stemming from a strong interference of the a_0 signal with the broad resonance $a_0(1450)$, which has a width of about 265 MeV. As a consequence the $a_0(980)$ maximum in the reaction $\bar{p}p \to \eta\pi^0\pi^0$ might be distorted. Moreover, the invariant-mass resolution in refs. [13,14] is only ~ 27 MeV/c^2.

In another recent study [15] the WA102 collaboration reported the branching ratio

$$\Gamma(a_0 \to K\bar{K})/\Gamma(a_0 \to \pi\eta) = 0.166 \pm 0.01 \pm 0.02, \quad (2)$$

[a] elena.bratkovskaya@theo.physik.uni-giessen.de

Reaction	R	M_r(GeV)	g_1(GeV)	Comment	Reference
$p\bar{p} \to \eta\pi^0\pi^0, \eta\eta\pi^0$	1.05–2.05	1.013–1.058	0.241–0.287	i)	[20]
$p\bar{p} \to \eta\pi^0\pi^0, \eta\eta\pi^0$	1.05–1.45	1.004–1.024	0.229–0.312	ii)	[20]
$p\bar{p} \to \eta\pi^0\pi^0, \eta\eta\pi^0$	1.12–1.37	0.999–1.006	0.211–0.275	iii)	[20]
$p\bar{p} \to \eta\pi^0\pi^0$	1.15±0.10	0.999±0.006	0.218±0.020	iv)	[14]
$p\bar{p} \to K_L K^+\pi^-$, $K_L K^-\pi^+$	1.03±0.4	0.999±0.002	0.324±0.015	v)	[13]
$\pi^- p \to n\eta\pi^-\pi^+, n\eta\pi^0$	0.91±0.10	1.001–0.0019	0.122±0.008	vi)	[11]

Table 1. Parameters of the Flatté parametrization for the $a_0(980)$. Comments: i) without any external constraint; ii) with constraint on $|a_0(980)|^2$ at half-width from the reaction $p\bar{p} \to \eta\omega\pi^0$; iii) with constraint on $|a_0(980)|^2$ at half-width from the reaction $p\bar{p} \to \eta\omega\pi^0$ and contribution from a hypothetical $a_2'(1620)$ in the fit; iv) solution B with constraint on the a_0 mass from the reaction $p\bar{p} \to \eta\omega\pi^0$; v) with constraint that the ratio of integrated intensities in the $K\bar{K}$ and $\eta\pi$ channels is given by eq. (1); vi) ref. [11] presents the value $g_{\pi\eta}$ =0.243±0.015 which is related to g_1 as $g_{\pi\eta} = (2/M)g_1$.

which was determined from the measured branching ratio for the $f_1(1285)$-meson,

$$\Gamma(f_1 \to K\bar{K}\pi)/\Gamma(f_1 \to \pi\pi\eta) = 0.166\pm0.01\pm0.08, \quad (3)$$

produced centrally in the reaction $pp \to p_f(X_0)p_s$ at 450 GeV/c. However, the authors assumed that the $f_1(1285)$ decays effectively by 100% to $a_0(980)\pi$ while the PDG quotes only a branching $\mathrm{Br}(f_1(1285) \to a_0(980)\pi) = 0.34 \pm 0.08$.

Therefore, it is necessary to measure the branching fractions of the two main a_0 decay channels ($\eta\pi$ and $K\bar{K}$) under different dynamical conditions with a higher mass resolution ($\Delta m < 10$ MeV/c^2) and lower background in an independent experiment. A related experiment to detect the a_0^+ in both main decay modes in the reaction $pp \to da_0^+$ will be performed at COSY (Jülich) [16]. An important dynamical feature of the latter reaction is that the production of the $a_0^+(980)$ near threshold cannot be related to an intermediate production of the $f_1(1285)$ (see below).

In this paper we investigate the a_0 production cross-section in the reactions $\pi N \to a_0 N$ and $pp \to da_0^+$ near threshold and at medium energies. In sect. 2 we present a short overview on the uncertainties of the a_0-decay parameters according to present knowledge. To analyze different contributions to the cross-section of the reaction $\pi N \to a_0 N$ we employ an effective Lagragian approach as well as the Regge-pole model in sect. 3. The results of this analysis then are used in sect. 4 to calculate the differential and total cross-sections of the reaction $pp \to da_0^+$ within the framework of the two-step model (TSM), in which two nucleons produce an a_0-meson via π-meson exchange and fuse to a deuteron. The TSM has been used before in refs. [17,18] for the analysis of η, η', ω and ϕ production in the reaction $pn \to dM$ near threshold. An important difference of our analysis here is that the S-wave channel in the reaction $pp \to da_0^+$ is forbidden due to angular-momentum conservation and the Pauli principle and that this reaction is dominated near threshold by the P-wave contribution. A summary of our work is presented in sect. 5.

2 Models and data on the K$\bar{\text{K}}$ and $\pi\eta$ decay channels of the $a_0(980)$

Within the framework of a coupled-channel formalism an appropriate parametrization of the shape of the $a_0(980)$ in each ($\eta\pi$ or $K\bar{K}$) channel can be taken in the form proposed by Flatté [19],

$$|A_i|^2 = \mathrm{Const}\frac{|\Gamma_i(M)|\ M_r^2}{(M^2 - M_r^2)^2 + M_r^2|\Gamma_{\mathrm{tot}}^2(M)|}\,, \quad (4)$$

where M_r is the K-matrix pole, $\Gamma_{\mathrm{tot}}(M) = \Gamma_1(M) + \Gamma_2(M) = g_1\rho_1 + g_2\rho_2$, while g_1 and g_2 are coupling constants to the two final states and ρ_i is given by the momenta of the final particles q_i as $\rho_i = 2q_i/M$. Note that molecular or "threshold cusp" cases would imply a dominance of the $|K\bar{K}\rangle$ component in Fock space and therefore correspond to a relatively large ratio $R = (g_2/g_1) \gg 1$. In table 1 we present the most recent results for the $a_0(980)$ parameters R, M_r and g_1, which show a sizeable variation especially in the coupling g_1 and ratio R, respectively.

In ref. [20] it has been shown that, when fitting the $\eta\pi$ mass distribution without any additional constraints, the parameters M_r, R and g_1 cannot be fixed very well. These parameters are strongly correlated and if one of them is moved in steps, the value of χ^2 changes rather slowly, but M_r, R and g_1 move together. Thus additional constraints are used in most fits. In ref. [11] a Breit-Wigner (BW) fit of the $a_0(980)$ shape in the $\eta\pi$ channel has been performed where the mass and width of the a_0^+ were determined to be 0.9964±0.0016 and 0.062±0.006 GeV/c^2, respectively. The two extractions of the a_0 mass and width (BW and Flatté) were found to be statistically consistent. Since in a Breit-Wigner parametrization only two parameters enter, it is not sensitive at all to the ratio R. This implies that for a reliable determination of R the measurements of both channels are necessary. Recall that two zero's of the function $D(M) = M^2 - M_r^2 + iM_r(g_1\rho_1(M) + g_2\rho_2(M))$ define two T-matrix poles on sheets II and III where only the position of the pole in sheet II defines the mass (m_0) and width (Γ_0) of the $a_0(980)$. Note that the pole mass m_0 is usually different from the resonance mass M_r in eq. (4). According to the PDG [10] the average value of the $a_0(980)$ mass is 0.9834 ± 0.0009 GeV/c^2 for the $\eta\pi$

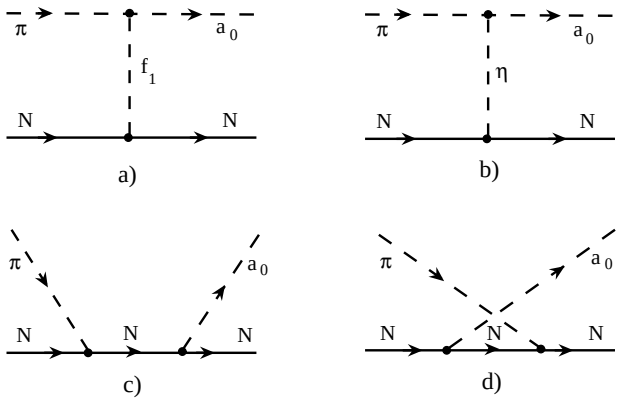

Fig. 1. The diagrams for a_0 production in the reaction $\pi N \to a_0 N$ near threshold.

final state (without the new result of the E852 Collaboration [11] (0.9983 ± 0.004 GeV/c^2)) and 0.9808 ± 0.0027 GeV/c^2 for the $K\bar{K}$ final state [13]. The width of the $a_0(980)$ is quoted as 0.092 ± 0.008 GeV in the $K\bar{K}$ final state [13] and 0.072 ± 0.01 GeV in the $\eta\pi$ final state [11].

The values of the ratio R presented in table 1 are not in favor of a pure molecular or pure "threshold cusp" interpretation of the $a_0(980)$. This statement is also in line with the results of ref. [3], where it was shown that the pure "threshold cusp" model gives an a_0 width of about 200 MeV, which is much larger than the experimental value. Nevertheless, there is still a comparatively large uncertainty in g_1 and g_2 : the values of g_1 may vary from 0.12 to 0.32 GeV and $R = g_2/g_1$ from 0.9 to 2.05. A better knowledge of g_1 and g_2 will help to understand the $a_0(980)$ internal structure or its decomposition in Fock space, respectively.

3 The reaction $\pi N \to a_0 N$

3.1 An effective Lagrangian Approach

The most simple mechanisms for a_0 production in the reaction $\pi N \to a_0 N$ near threshold are described by the pole diagrams shown in fig. 1 a–d. It is known experimentally that the a_0 couples strongly to the channels $\pi\eta$ and $\pi f_1(1285)$ because $\pi\eta$ is the dominant decay channel of the a_0 while πa_0 is one of the most important decay channels of the $f_1(1285)$ [10]. The amplitudes, which correspond to the t-channel exchange of $\eta(550)$- and $f_1(1285)$- mesons (a,b), can be written as

$$M^t_\eta(\pi^- p \to a_0^- p) = g_{\eta\pi a_0} g_{\eta NN}\ \bar{u}(p_2')\gamma_5 u(p_2) \times \frac{1}{t - m_\eta^2}\ F_{\eta\pi a_0}(t) F_{\eta NN}(t)\,, \tag{5}$$

$$M^t_{f_1}(\pi^- p \to a_0^- p) = g_{f_1\pi a_0} g_{f_1 NN} \times (p_1 + p_1')_\mu \left(g_{\mu\nu} - \frac{q_\mu q_\nu}{m_{f_1}^2}\right) \bar{u}(p_2')\gamma_\nu\gamma_5 u(p_2) \times \frac{1}{t - m_{f_1}^2}\ F_{f_1\pi a_0}(t) F_{f_1 NN}(t). \tag{6}$$

Here p_1 and p_1' are the four momenta of π^-, a_0^-, whereas p_2 and p_2' are the four momenta of the initial and final protons, respectively; furthermore, $q = p_2' - p_2$, $t = (p_2' - p_2)^2$. The functions F_j present form factors at the different vertices j ($j = f_1 NN, \eta NN$), which are taken of the monopole form

$$F_j(t) = \frac{\Lambda_j^2 - m_j^2}{\Lambda_j^2 - t}, \tag{7}$$

where Λ_j is a cut-off parameter. In the case of η exchange we use $g_{\eta NN} = 3$, $\Lambda_{\eta NN}$=1.5 GeV from ref. [21] and $g_{\eta\pi a_0}$=2.46 GeV which results from the width $\Gamma(a_0 \to \eta\pi) = 80$ MeV. The contribution of the f_1 exchange is calculated for two parameter sets; set A: $g_{f_1 NN} = 11.2$, $\Lambda_{f_1 NN} = 1.5$ GeV from ref. [22], set B: $g_{f_1 NN} = 14.6$, $\Lambda_{f_1 NN} = 2.0$ GeV from ref. [23] and $g_{f_1\pi a_0}$=2.5 for both cases. The latter value for $g_{f_1 a_0\pi}$ corresponds to $\Gamma(f_1 \to a_0\pi) = 24$ MeV and $\mathrm{Br}(f_1 \to a_0\pi) = 34\%$.

In fig. 2 (upper part) we show the differential cross-sections $\mathrm{d}\sigma/\mathrm{d}t$ for the reaction $\pi^- p \to a_0^- p$ at 2.4 GeV/c corresponding to η (dash-dotted) and f_1 exchanges with set A (solid line) and set B (dashed line). A soft cut-off parameter (set A) close to the mass of the f_1 implies that all the contributions related to f_1 exchange become negligibly small. On the other hand, for the parameter values given by set B, the f_1 exchange contribution is much larger than that from η exchange. Note, that this large uncertainty in the cut-off presently cannot be controlled by data and we will discuss the relevance of the f_1 exchange contribution for all reactions separately throughout this study. For set B the total cross-section for the reaction $\pi^- p \to a_0^- p$ can be about 0.5 mb at 2.4 GeV/c (cf. fig. 3 (upper part)) while the forward differential cross-section can be about 1 mb/GeV^2.

The η and f_1 exchanges, however, do not contribute to the amplitude of the charge exchange reaction $\pi^- p \to a_0^0 n$. In this case we have to consider the contributions of the s- and u-channel diagrams (fig. 1 c and d):

$$M^s_N(\pi^- p \to a_0^0 n) = \sqrt{2} g_{a_0 NN} \frac{f_{\pi NN}}{m_\pi}\ \frac{1}{s - m_N^2} F_N(s) \times p_{1\mu}\ \bar{u}(p_2')\left[(p_1 + p_2)_\alpha \gamma_\alpha + m_N\right]\gamma_\mu\ \gamma_5 u(p_2)\,, \tag{8}$$

$$M^u_N(\pi^- p \to a_0^0 n) = \sqrt{2} g_{a_0 NN} \frac{f_{\pi NN}}{m_\pi}\ \frac{1}{u - m_N^2} F_N(u) \times p_{1\mu}\ \bar{u}(p_2')\gamma_\mu\gamma_5\left[(p_2 - p_1')_\alpha \gamma_\alpha + m_N\right] u(p_2), \tag{9}$$

where $s = (p_1 + p_2)^2$, $u = (p_2 - p_1')^2$ and m_N is the nucleon mass.

The πNN coupling constant is taken as $f^2_{\pi NN}/4\pi = 0.08$ [21] and the form factor for each virtual nucleon is taken in the form [24]

$$F_N(u) = \frac{\Lambda_N^4}{\Lambda_N^4 + (u - m_N^2)^2} \tag{10}$$

with a cut-off parameter $\Lambda_N = 1.2$–1.3 GeV.

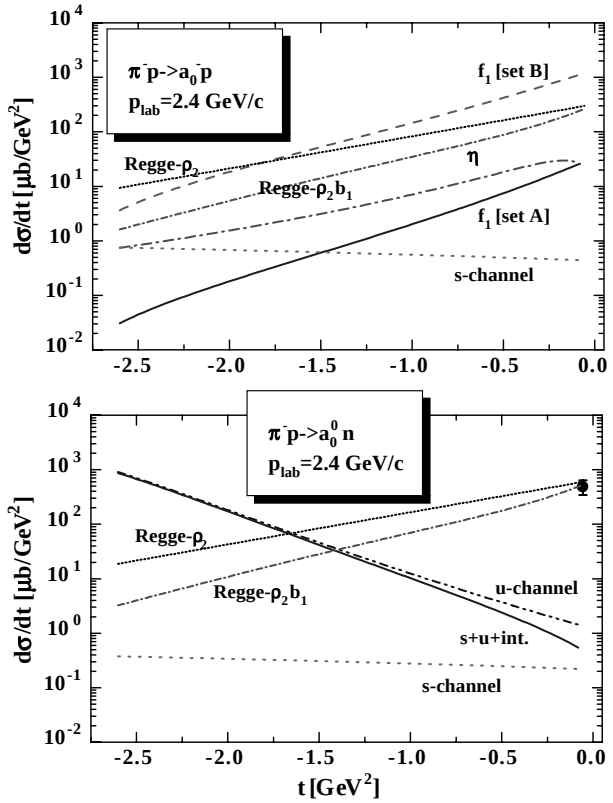

Fig. 2. The differential cross-sections $d\sigma/dt$ for the reactions $\pi^- p \to a_0^- p$ (upper part) and $\pi^- p \to a_0^0 n$ (lower part) at 2.4 GeV/c. The dash-dotted line corresponds to the η exchange, solid and dashed lines (upper part) show the f_1 contributions within sets A and B, respectively. The dotted and dash–double-dotted lines indicate the s- and u-channels while the solid line (lower part) describes the coherent sum of s- and u- channel contributions. The short dotted and short dash-dotted lines present the results within the ρ_2 and (ρ_2, b_1) Regge exchange model, respectively (see text). The experimental point is taken from ref. [28].

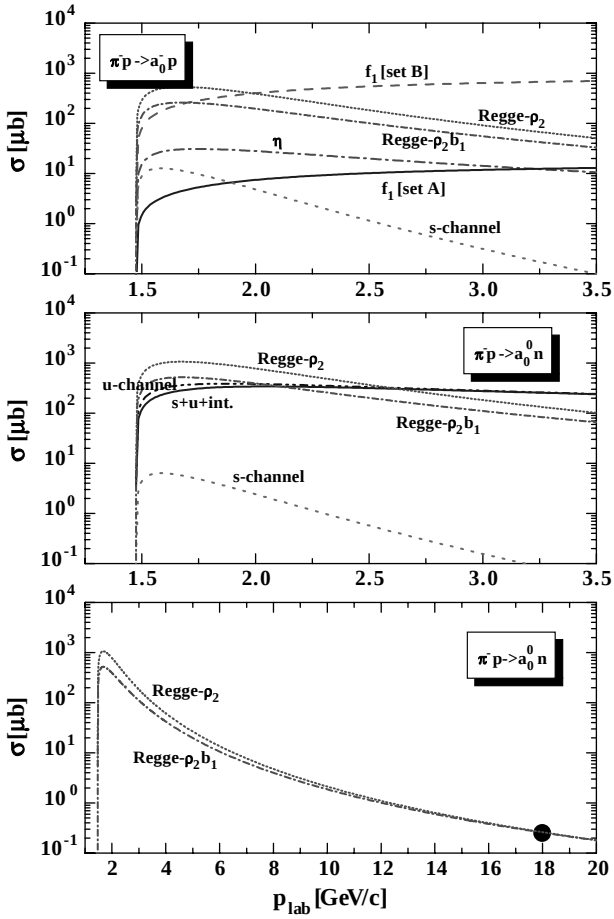

Fig. 3. The total cross-sections for the reactions $\pi^- p \to a_0^- p$ (upper part) and $\pi^- p \to a_0^0 n$ (middle and lower part) as a function of the incident momentum. The assignment of the lines is the same as in fig. 2. The experimental data point at 18 GeV/c (lower part) is taken from ref. [34].

The dotted and dash–double-dotted lines in the lower part of fig. 2 show the differential cross-section for the charge exchange reaction $\pi^- p \to a_0^0 n$ at 2.4 GeV/c corresponding to s- and u-channel diagrams, respectively. Due to isospin only the s-channel contributes to the $\pi^- p \to a_0^- p$ reaction (dotted line in the upper part of fig. 2). In these calculations the cut-off parameter $\Lambda_N = 1.24$ GeV and $g^2_{a_0 NN}/4\pi$=1.075 is taken from ref. [23]. The solid line in the lower part of fig. 2 describes the coherent sum of the s- and u-channel contributions. Except for the very forward region the s-channel contribution (dotted line) is rather small compared to the u-channel for the charge exchange reaction $\pi^- p \to a_0^0 n$, which may give a backward differential cross-section of about 1 mb/GeV^2 . The corresponding total cross-section can be about 0.3 mb at this energy (cf. fig. 3, middle part).

Unfortunately, there are no experimental data for the total cross-section of a_0 production in πN collisions near the threshold. Some crude estimates can only be done by comparing the a_0 production with ρ and ω production. For example, the WA57 collaboration has measured inclusive photoproduction of $a_0^{\pm}(980)$ mesons at photon energies of 25–55 GeV [25]. It was found that the cross-section of this process is rather large and about $\sim 1/6$ of the cross-sections for the corresponding non-diffractive production of leading ρ^0, ω, ρ^+ and ρ^- mesons. Furthermore, in the LBL experiment [26] the measured cross-sections $d\sigma/d\Omega$ for the reaction $pp \to d a_0^+(980)$ at 3.8–6.3 GeV/c are $\sim$ (1/4–1/6) of the cross-section for ρ^+ production (table 2).

$pp \to d\rho^+$	3.8 GeV/c	4.5 GeV/c	6.3 GeV/c
$d\sigma/d\Omega(\mu b/sr)$	3.2±0.5	2.0±0.4	0.5±0.5
$pp \to d a_0^+(980)$	3.8 GeV/c	4.5 GeV/c	6.3 GeV/c
$d\sigma/d\Omega(\mu b/sr)$	$0.5^{+0.7}_{-0.15}$	$0.48^{+0.28}_{-0.15}$	$0.35^{+0.10}_{-0.15}$

Table 2. cross-sections for the reactions $pp \to d a_0^+(980)$ and $pp \to d\rho^+$ from ref. [26].

In view of these arguments we also compare the cross-sections for the reactions $\pi^- p \to a_0^0 n$ and $\pi^- p \to \rho^0(\omega) n$

at 2.4 GeV/c. According to the parametrization of ref. [27] we have $\sigma(\pi^- p \to \rho^0 n) \approx 2\sigma(\pi^- p \to \omega n) \approx 1.8$ mb; our estimate then gives $\sigma(\pi^- p \to a_0^0 n) \approx 0.15$–$0.3$ mb, which is in a reasonable agreement with the u-channel mechanism as well as f_1 exchange contribution with parameters from set B (cf. fig. 3).

There is a single experimental point for the forward differential cross-section of the reaction $\pi^- p \to a_0^0 n$ at 2.4 GeV/c (ref. [28], lower part of fig. 2),

$$\left.\frac{\mathrm{d}\sigma}{\mathrm{d}t}(\pi^- p \to a_0^0 n)\right|_{t\approx 0} = 0.49 \text{ mb/GeV}^2.$$

Since in the forward region ($t \approx 0$) the s- and u-channel diagrams only give a smaller cross-section, the charge exchange reaction $\pi^- p \to a_0^0 n$ is most probably dominated at small t by the isovector $b_1(1^{+-})$- and $\rho_2(2^{--})$-meson exchanges (see, *e.g.*, ref. [29]). Though the couplings of these mesons to πa_0 and NN are not known, we can estimate $\frac{\mathrm{d}\sigma}{\mathrm{d}t}(\pi^- p \to a_0^0 n)$ in the forward region using the Regge-pole model as developed by Achasov and Shestakov [29]. Note, that the Regge-pole model is expected to provide a reasonable estimate for the cross-section at medium energies of about a few GeV and higher (see, *e.g.*, refs. [30, 31] and references therein).

3.2 The Regge-pole model

The s-channel helicity amplitudes for the reaction $\pi^- p \to a_0^0 n$ can be written as

$$M_{\lambda_2'\lambda_2}(\pi^- p \to a_0^0 n) = \bar{u}_{\lambda_2'}(p_2') \times \left[-A(s,t) + (p_1 + p_1')_\alpha \gamma_\alpha \frac{B(s,t)}{2}\right] \gamma_5 u_{\lambda_2}(p_2), \quad (11)$$

where the invariant amplitudes $A(s,t)$ and $B(s,t)$ do not contain kinematical singularities and (at fixed t and large s) are related to the helicity amplitudes as

$$M_{++} \approx -sB, \quad M_{+-} \approx \sqrt{t_{\min} - t}\, A. \quad (12)$$

The differential cross-section then can be expressed through the helicity amplitudes in the standard way as

$$\frac{\mathrm{d}\sigma}{\mathrm{d}t}(\pi^- p \to a_0^0 n) = \frac{1}{64\pi s}\frac{1}{(p_1^{\mathrm{cm}})^2}(|M_{++}|^2 + |M_{+-}|^2). \quad (13)$$

Usually it is assumed that the reaction $\pi^- p \to a_0^0 n$ at high energies is dominated by the b_1 Regge-pole exchange. However, as shown by Achasov and Shestakov [29] this assumption is not compatible with the angular dependence of $\mathrm{d}\sigma/\mathrm{d}t(\pi^- p \to a_0^0 n)$ observed at Serpukhov at 40 GeV/c [32,33] and Brookhaven at 18 GeV/c [34]. The reason is that the b_1 Regge trajectory contributes only to the amplitude $A(s,t)$ giving a dip in differential cross-section at forward angles, while the data show a clear forward peak in $\mathrm{d}\sigma/\mathrm{d}t(\pi^- p \to a_0^0 n)$ at both energies. To interpret this phenomenon Achasov and Shestakov introduced a ρ_2 Regge-pole exchange conspiring with its daughter trajectory. Since the ρ_2 Regge trajectory contributes to both invariant amplitudes, $A(s,t)$ and $B(s,t)$, its contribution does not vanish at $\Theta = 0$ thus giving a forward peak due to the term $|M_{++}|^2$ in $\mathrm{d}\sigma/\mathrm{d}t$. At the same time the contribution of the ρ_2 daughter trajectory to the amplitude $A(s,t)$ is necessary to cancel the kinematical pole at $t = 0$ introduced by the ρ_2 main trajectory (conspiracy effect). In this model the s-channel helicity amplitudes can be expressed through the b_1 and the conspiring ρ_2 Regge trajectories exchange as

$$M_{++} \approx M_{++}^{\rho_2}(s,t) = \gamma_{\rho_2}(t) \exp[-i\frac{\pi}{2}\alpha_{\rho_2}(t)] \left(\frac{s}{s_0}\right)^{\alpha_{\rho_2}(t)}, \quad (14)$$

$$M_{+-} \approx M_{+-}^{b_1}(s,t) = \sqrt{(t_{\min} - t)/s_0}\ \gamma_{b_1}(t) \times i \exp[-i\frac{\pi}{2}\alpha_{b_1}(t)] \left(\frac{s}{s_0}\right)^{\alpha_{b_1}(t)}, \quad (15)$$

where $\gamma_{\rho_2}(t) = \gamma_{\rho_2}(0)\exp(b_{\rho_2} t)$, $\gamma_{b_1}(t) = \gamma_{b_1}(0)\exp(b_{b_1} t)$, $t_{\min} \approx -m_N^2(m_{a_0}^2 - m_\pi^2)^2/s^2$, $s_0 \approx 1$ GeV^2, while the meson Regge trajectories have the linear form $\alpha_j(t) = \alpha_j(0) + \alpha_j'(0)t$.

Achasov and Shestakov describe the Brookhaven data on the t distribution at 18 GeV/c for $-t_{\min} \le -t \le 0.6$ GeV^2 [34] by the expression

$$\frac{\mathrm{d}N}{\mathrm{d}t} = C_1 \left[e^{\Lambda_1 t} + (t_{\min} - t)\frac{C_2}{C_1} e^{\Lambda_2 t}\right], \quad (16)$$

where the first and second terms describe the ρ_2 and b_1 exchanges, respectively. They found two fits: a) $\Lambda_1 = 4.7$ GeV$^{-2}, C_2/C_1 = 0$; b) $\Lambda_1 = 7.6$ GeV$^{-2}, C_2/C_1 \approx 2.6$ GeV$^{-2}, \Lambda_2 = 5.8$ GeV^{-2}. This implies that the b_1 contribution is equal to zero for fit a) and yields only 1/3 of the integrated cross-section for fit b) at 18 GeV/c. Moreover, using the available data on the reaction $\pi^- p \to a_2^0(1320)n$ at 18 GeV/c and comparing them with the data on the $\pi^- p \to a_0^0 n$ reaction they estimated the total and forward differential cross-sections $\sigma(\pi^- p \to a_0^0 n \to \pi^0\eta n) \approx 200$ nb and $[\mathrm{d}\sigma/\mathrm{d}t(\pi^- p \to a_0^0 n \to \pi^0\eta n)]_{t=0} \approx 940$ nb/GeV^2. Taking $\mathrm{Br}(a_0^0 \to \pi^0\eta) \approx 0.8$ we find $\sigma(\pi^- p \to a_0^0 n) \approx 0.25$ μb and $[\mathrm{d}\sigma/\mathrm{d}t(\pi^- p \to a_0^0 n)]_{t=0} \approx 1.2$ μb/GeV^2. In this way all the parameters of the Regge model can be fixed and we will employ it for the energy dependence of the $\pi^- p \to a_0^0 n$ cross-section to obtain an estimate at lower energies, too.

The mass of the $\rho_2(2^{--})$ is expected to be about 1.7 GeV (see [35] and references therein) and the slope of the meson Regge trajectory in the case of light (u,d)-quarks is 0.9 GeV^{-2} [36]. Therefore, the intercept of the ρ_2 Regge trajectory is $\alpha_{\rho_2}(0) = 2 - 0.9 m_{\rho_2}^2 \approx -0.6$. Similarly — in the case of the b_1 trajectory — we have $\alpha_{b_1}(0) \approx -0.37$. At forward angles we can neglect the contribution of the b_1 exchange (see discussion above) and write the energy dependence of the differential cross-section in the form

$$\left.\frac{\mathrm{d}\sigma_{\mathrm{Regge}}}{\mathrm{d}t}(\pi^- p \to a_0^0 n)\right|_{t=0} \approx \left.\frac{\mathrm{d}\sigma_{\rho_2}}{\mathrm{d}t}\right|_{t=0} \sim \sim \frac{1}{(p_1^{\mathrm{cm}})^2}\left(\frac{s}{s_0}\right)^{-2.2}. \quad (17)$$

This provides the following estimate for the forward differential cross-section at 2.4 GeV/c,

$$\frac{\mathrm{d}\sigma_{\mathrm{Regge}}}{\mathrm{d}t}(\pi^- p \to a_0^0 n)\bigg|_{t=0} \approx 0.6 \text{ mb/GeV}^2, \qquad (18)$$

which is in agreement with the experimental data point [28] (lower part of fig. 2). Since the b_1 and ρ_2 Regge trajectories have isospin 1, their contribution to the cross-section for the reaction $\pi^- p \to a_0^- p$ is twice smaller,

$$\frac{\mathrm{d}\sigma_{\mathrm{Regge}}}{\mathrm{d}t}(\pi^- p \to a_0^- p) = \frac{1}{2}\,\frac{\mathrm{d}\sigma_{\mathrm{Regge}}}{\mathrm{d}t}(\pi^- p \to a_0^0 n). \qquad (19)$$

In fig. 2 the short-dotted lines show the resulting differential cross-sections for $\mathrm{d}\sigma_{\mathrm{Regge}}(\pi^- p \to a_0^- p)/\mathrm{d}t$ (upper part) and $\mathrm{d}\sigma_{\mathrm{Regge}}(\pi^- p \to a_0^0 n)/\mathrm{d}t$ (lower part) at 2.4 GeV/c corresponding to ρ_2 Regge exchange (fit a)), whereas the dash-dotted lines indicate the contribution for ρ_2 and b_1 Regge trajectories (fit b)). For $t \to 0$ both Regge parametrizations agree, however, at large $|t|$ the solution including the b_1 exchange gives a smaller cross-section. The cross-section $\mathrm{d}\sigma_{\mathrm{Regge}}(\pi^- p \to a_0^- p)/\mathrm{d}t$ in the forward region exceeds the contributions of η, f_1 (set A) and s-channel exchanges, however, is a few times smaller than the f_1 exchange contribution for set B. On the other hand, the cross-section $\mathrm{d}\sigma_{\mathrm{Regge}}(\pi^- p \to a_0^0 n)/\mathrm{d}t$ is much larger than the s- and u-channel contributions in the forward region, but much smaller than the u-channel contribution in the backward region.

The integrated cross-sections for $\pi^- p \to a_0^- p$ (upper part) and $\pi^- p \to a_0^0 n$ (middle and lower part) for the Regge model are shown in fig. 3 as a function of the pion laboratory momentum by short-dotted lines for ρ_2 exchange and by short dash-dotted lines for ρ_2, b_1 trajectories. In the few GeV region the cross-sections are comparable with the u-channel and f_1-exchange contribution (set B). At higher energies it decreases as $s^{-3.2}$ in contrast to the non-Reggeized u-channel and f_1- exchange contributions which anyhow should only be employed close to the threshold region.

The main conclusions of this section are as follows: In the region of a few GeV the dominant mechanisms of a_0 production in the reaction $\pi N \to a_0 N$ are u-channel nucleon and t-channel f_1 -meson exchanges which give cross-sections for a_0 production about 0.3–0.4 mb (cf. upper part of fig. 3). Similar cross-sections ($\simeq$ 0.4–1 mb) are predicted by the Regge model with conspiring ρ_2 (or ρ_2 and b_1) exchanges, normalized to the Brookhaven data at 18 GeV/c (lower part of fig. 3). The contributions of s-channel nucleon and t-channel η-meson exchanges are small (cf. upper and middle parts of fig. 3).

4 The reaction pp → da$_0^+$

The missing mass spectrum in the reaction $pp \to dX$ for deuterons produced at 0° in the laboratory and incident momenta of 3.8, 4.5 and 6.3 GeV/c has been measured at LBL (Berkeley) [26]. It is interesting, that apart from the missing mass peaks corresponding to π and ρ production, there is a distinctive structure in the missing mass spectrum at 0.95 GeV^2, which was identified as a_0 production.

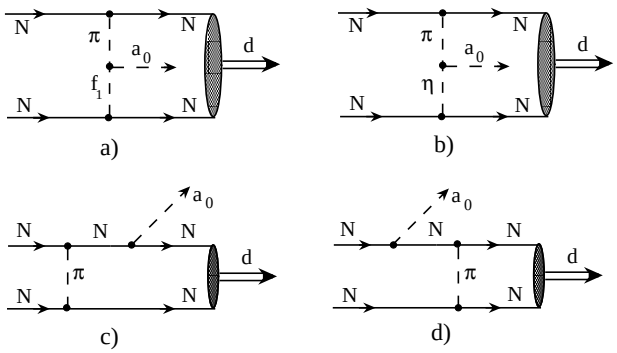

Fig. 4. The diagrams describing the different mechanisms of the a_0-meson production in the reaction $NN \to da_0$ within the framework of the two-step model (TSM).

In order to estimate the cross-section for the reaction $pp \to da_0^+$ at lower momenta (available at COSY) we use the two-step model (TSM) (cf. refs. [17,18]). The contributions of hadronic intermediate states to the P-wave amplitude of the reaction $pp \to da_0^+$ (within the framework of the TSM) are described by the diagrams a-d in fig. 4. We consider three different contributions from the amplitude $\pi N \to a_0 N$: i) the $f_1(1285)$- meson exchanges (fig. 4 a); ii) the η- meson exchange (fig. 4 b); iii) s- and u-channel nucleon exchanges (fig. 4 c and d). As follows from the analysis in sect. 3 the contributions of the η-exchange and s-channel nucleon can be neglected. We thus restrict to the f_1-exchange (set B) and the u-channel nucleon current.

The cut-off Λ_N for nucleon exchange (eq. (10)) is considered as a free parameter now within the interval 1.2–1.3 GeV. In order to preserve the correct structure of the amplitude under permutations of the initial nucleons (which are antisymmetric in the isovector state) the amplitude is written as the difference of t- and u-channel contributions in the form

$$T^{\pi}_{pp\to dM}(s,t,u) = A_{pp\to dM}(s,t) - A_{pp\to dM}(s,u), \qquad (20)$$

where M stands for the a_0^+-meson. Furthermore, $s = (p_1 + p_2)^2$, $t = (p_3 - p_1)^2$, $u = (p_3 - p_2)^2$ where p_1, p_2, p_3, and p_4 are the 4-momenta of the initial protons, meson M and the deuteron, respectively. The structure of the amplitude (20) guarantees that the S-wave part vanishes since it is forbidden by angular-momentum conservation and the Pauli principle.

Since we are interested in the $pp \to da_0^+$ cross-section near threshold, where the momentum of the deuteron is comparatively small, we use a non-relativistic description of this particle by neglecting the 4th component of its polarization vector. Correspondingly, the relative motion of nucleons in the deuteron is also treated non-relativistically. Then one can write the first (t-channel)

term on the r.h.s. of eq. (20) as ([17])

$$A_{pp\to da_0^+}(s,t) = \frac{f_{\pi NN}}{m_\pi}\; g_{f_1 NN}\; g_{f_1\pi a_0} \times \sqrt{(p_1^0+m_N)(p_2^0+m_N)} \times M^{jl}(\mathbf{p}_1,\mathbf{p}_3)\; \varphi^T_{\lambda_2}(\mathbf{p}_2)\; (-i\sigma_2)\sigma^j\sigma\cdot\epsilon^{\,*(d)}\sigma^l\varphi_{\lambda_1}(\mathbf{p}_1), \tag{21}$$

where $\epsilon^{\,(d)}$ is the polarization vector of the deuteron; $p_1^0 = p_2^0 = \sqrt{\mathbf{p}_1^2+m_N^2}$, while φ_λ are the (2-component) spinors of the nucleons in the initial state. The tensor function $M^{jl}(\mathbf{p}_1,\mathbf{p}_3)$ is defined by the integral

$$M^{jl}(\mathbf{p}_1,\mathbf{p}_3) = \sqrt{2m_N}\int \frac{\mathrm{d}^3p_2'}{(2\pi)^{3/2}} \times \sqrt{(p_1'^0+m_N)(p_2'^0+m_N)}\;\left\{\frac{p_1^j}{p_1^0+m_N}+\frac{p_2'^j}{p_2'^0+m_N}\right\} \times I\cdot\Phi^l_{\pi^0N\to a_0^0N}(\mathbf{p}_2',\mathbf{p}_1,\mathbf{p}_3)\;\frac{F_{\pi NN}(q_\pi^2)}{q_\pi^2-m_\pi^2}\;\Psi_d(\mathbf{p}_2'+\mathbf{p_3}/2), \tag{22}$$

where the contribution of f_1- exchange is given by

$$\Phi^l_{\pi^0N\to a_0^0N(f_1)}(\mathbf{p}_2',\mathbf{p}_1,\mathbf{p}_3) = g_{f_1NN}\; g_{f_1\pi a_0}\;\frac{F_{f_1NN}(q_{f_1}^2)}{q_{f_1}^2-m_{f_1}^2} \times\left\{2p_3^l-\frac{2(p_3+p_2')^l}{p_1'^0+m_N}\;\left(m_N\left[1+\frac{m_{a_0}^2-q_2^2}{m_{f_1}^2}\right]-p_3^0\right) - \frac{2p_1^l}{p_1^0+m_N}\;\left(m_N\left[1+\frac{m_{a_0}^2-q_2^2}{m_{f_1}^2}\right]+p_3^0\right)\right\}. \tag{23}$$

The u-channel contribution reads

$$\Phi^l_{\pi^0N\to a_0^0N(u)}(\mathbf{p}_2',\mathbf{p}_1,\mathbf{p}_3) = g_{a_0NN}\;\frac{f_{\pi NN}}{m_\pi}\;2m_N \times\left\{-p_3^l+\frac{(p_3+p_2')^l}{p_1'^0+m_N}\;\left(\frac{m_N}{2}\;\left[3+\frac{q_N^2}{m_N^2}\right]-p_3^0\right) + \frac{p_1^l}{p_1^0+m_N}\;\left(\frac{m_N}{2}\;\left[3+\frac{q_N^2}{m_N^2}\right]+p_3^0\right)\right\}\;\frac{F_N(q_N^2)}{q_N^2-m_N^2}. \tag{24}$$

Here $\Psi_d(\mathbf{p}_2'+\mathbf{p_3}/2)$ is the deuteron wave function for which we use the Paris model [37]. In (22) I is the isospin factor which depends on the mechanism of the reaction $pp \to (pn)a_0^+$. For f_1 and u-channel exchange we have $I_{(f_1)} = 1$ and $I_{(u)} = 3\sqrt{2}$, respectively. Further kinematical quantities, which also dependent on the momenta $\mathbf{p}_1$, $\mathbf{p}_3$ and $\mathbf{p}_2'$, are defined as

$$\begin{aligned}
q_\pi^2 &= -\delta_0(\mathbf{p}_2'^2+\beta_\pi(\mathbf{p}_1)) - 2\mathbf{p}_1\mathbf{p}_2',\\
q_{f_1}^2 &= -\delta_0\left(\mathbf{p}_2'^2+\beta_{f_1}(\mathbf{p}_1,\mathbf{p}_3)\right)+\frac{p_3^0}{m_N}\;\mathbf{p}_2'^2\\
&\quad -2\mathbf{p}_1\cdot\mathbf{p}_2' - 2\mathbf{p}_3\cdot\mathbf{p}_2' - 2\mathbf{p}_3\cdot\mathbf{p}_1,\\
q_N^2 &= m_N^2+m_{a_0}^2-2p_1^0p_3^0+2\mathbf{p}_1\cdot\mathbf{p}_3,\\
\beta_\pi(\mathbf{p}_1) &= (\mathbf{p}_1^2-T_1^2)/\delta_0,\\
\beta_{f_1}(\mathbf{p}_1,\mathbf{p}_3) &= \beta_\pi(\mathbf{p}_1) - m_{a_0}^2/\delta_0 + p_3^0m_N\\
\delta_0 &= p_1^0/m_N,\quad T_1 = \sqrt{\mathbf{p}_1^2+m_N^2}-m_N\;,\\
p_2'^0 &= \sqrt{\mathbf{p}_2'^2+m_N^2},\quad p_3^0 = \sqrt{\mathbf{p}_3^2+m_{a_0}^2},\\
p_1'^0 &= \sqrt{(\mathbf{p}_2'+\mathbf{p}_3)^{\,2}+m_N^2}.
\end{aligned} \tag{25}$$

with m_{a_0} denoting the mass of the a_0-meson. The form factors F_{f_1NN} and $F_{\pi NN}$ are taken in the form (7) within $\Lambda_{\pi NN} = 1.3$ GeV for the πNN vertex according to ref. [21] and parameter set B for the f_1NN vertex. The u-channel term $A_{pp\to da_0^+}(s,u)$ in eq. (20) can be obtained from (21) by the substitution $p_1 \leftrightarrow p_2$, $\varphi_{\lambda_1} \leftrightarrow \varphi_{\lambda_2}$.

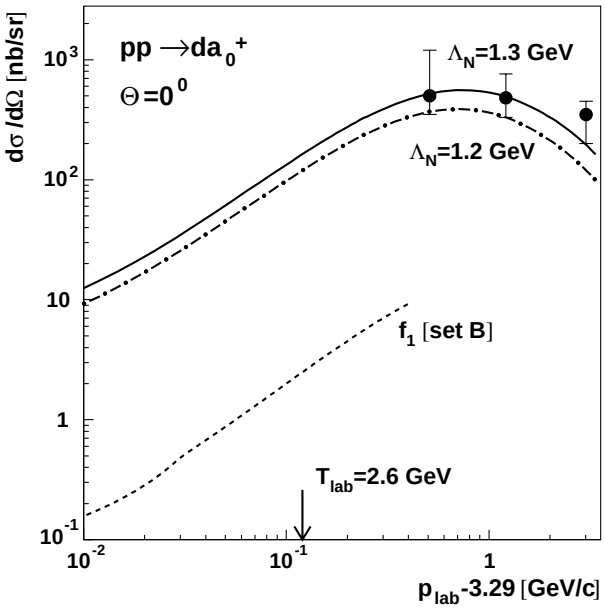

Fig. 5. Forward differential cross-section of the reaction $pp \to da_0^+$ as a function of $(p_{\rm lab}-3.29)$ GeV/c. The full dots are the experimental data from ref. [26]. The dash-dotted and solid lines describe the results of the TSM calculated at $\Lambda_N = 1.2$ and 1.3 GeV, respectively. The dotted line shows the contribution of f_1 exchange for the parameter set B (see text).

The differential cross-section $pp \to da_0^+$ then can be written as

$$\frac{\mathrm{d}\sigma_{pp\to da_0^+}}{\mathrm{d}t} = \frac{1}{64\pi s}\;\frac{1}{(p_1^{\rm cm})^2} \times\overline{|A_{pp\to da_0^+}(s,t)-A_{pp\to da_0^+}(s,u)|^2}. \tag{26}$$

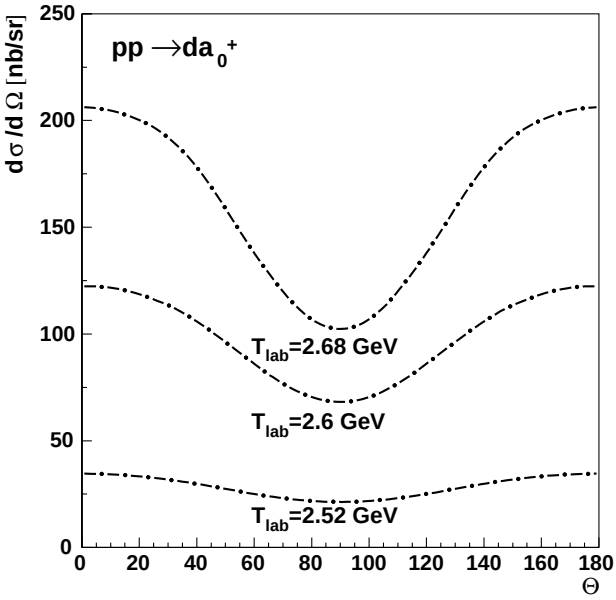

Fig. 6. Angular dependence of the differential cross-section $\mathrm{d}\sigma/\mathrm{d}\Omega$ of the reaction $pp \to da_0^+$ in the c.m.s. at different energies. The cut-off parameter for the u-channel nucleon exchange is $\Lambda_N = 1.3$ GeV.

The calculated forward differential cross-section (as a function of the proton-beam momentum) is presented in fig. 5. The dash-dotted and solid lines describe the results of the TSM for different values of the nucleon cut-off parameter: $\Lambda_N = 1.2$ and 1.3 GeV, respectively. A rather good description of the existing data [26] is achieved for $\Lambda_N = 1.3$ GeV (solid line). We recall that in sect. 3 we have used $\Lambda_N = 1.24$ GeV from ref. [23] which gives a cross-section in between the dash-dotted and solid line. Our predictions for this cross-section practically do not depend on the couplings of the f_1 since the f_1 exchange contribution turns out to be very small even for parameter set B (dashed line in fig. 5). The arrow in fig. 5 indicates the maximum proton momentum presently available at COSY. At this energy a differential cross-section of 0.1–0.2 μb/sr should be expected according to our calculations.

In fig. 6 the calculated angular differential cross-section for the reaction $pp \to da_0^+$ is shown as a function of the center-of-mass angle Θ which can be parametrized as

$$\frac{\mathrm{d}\sigma}{\mathrm{d}\Omega} = A + B \cdot \cos^2\Theta + C \cdot \cos^4\Theta. \qquad (27)$$

The results of our calculations in the framework of the TSM for $\Lambda_N = 1.3$ GeV are:
$A = 21.3$ nb/sr, $B = 15.3$ nb/sr, $C = -2.1$ nb/sr
at $T_{\mathrm{lab}} = 2.52$ GeV ($\sigma_{\mathrm{tot}} = 330$ nb);
$A = 68$ nb/sr, $B = 76$ nb/sr, $C = -22$ nb/sr
at $T_{\mathrm{lab}} = 2.6$ GeV ($\sigma_{\mathrm{tot}} = 1120$ nb);
$A = 78$ nb/sr, $B = 97$ nb/sr, $C = -31$ nb/sr
at $T_{\mathrm{lab}} = 2.62$ GeV ($\sigma_{\mathrm{tot}} = 1310$ nb).

We note that an understanding of the $a_0(980)$ production mechanism may also give interesting information on its internal structure. For example, the WA57 collaboration has interpreted the relatively strong production of the $a_0^{\pm}(980)$ in photon induced reactions at energies of 25–55 GeV as evidence for a $q\bar{q}$ state rather than a $qq\bar{q}\bar{q}$ state [25]. This argument can also be used here. If measurements at COSY will confirm a comparatively large value of the $a_0^+(980)$ production cross-section as presented in this work, this will provide further evidence that the $a_0^+(980)$ has an essential admixture of a $q\bar{q}$ component.

5 Conclusions

In this work we have estimated a_0 production cross-sections in the reaction $\pi N \to a_0 N$ near threshold and at medium energies by considering the $a_0(980)$-resonance as a usual $q\bar{q}$-meson. Using an effective Lagragian approach we have analyzed different contributions to the differential and total cross-sections, *i.e.* t-channel η- and f_1-meson exchanges as well as s- and u-channel nucleon exchanges, and have found that the f_1- and u-channel contributions are dominant in the $\pi^- p \to a_0^- p$ and $\pi^- p \to a_0^0 n$ reactions, respectively. We have analyzed also predictions of the Regge model with conspiring ρ_2 exchange normalized to the data at 18 GeV/c. We found that this model gives (in the few GeV region) a cross-section comparable to the f_1- and u-channel mechanisms.

The latter results have been used to calculate the differential and total cross-section of the reaction $pp \to da_0^+$ within the framework of the two-step model, where the amplitude of the $NN \to da_0$ reaction can be expressed through the amplitude of the $\pi N \to a_0 N$ reaction and a structure integral containing the deuteron wave function in the non-relativistic limit. It is found that the cross-section of the $pp \to da_0^+$ reaction is dominated almost entirely by the u-channel mechanism reaching a value of about 1 μb at $T_{\mathrm{lab}} = 2.6$ GeV. An experimental confirmation of this comparatively large production cross-section would imply that the $a_0^+(980)$ has an essential admixture of a $q\bar{q}$ component.

We are grateful to A. Sibirtsev for helpful discussions. This work has been supported by DFG, RFFI and GSI Darmstadt.

References

1. F.E. Close et al., Phys. Lett. B **319**, 291 (1993); hep-ph/0006288.
2. M. Genovese et al., Nuovo Cim. A **107**, 1249 (1994).
3. G. Janssen, B. Pierce, K. Holinde and J. Speth, Phys. Rev. D **52**, 2690 (1995).
4. V.V. Anisovich et al., Phys. Lett. B **355**, 363 (1995).
5. K. Maltman, *Proc. 8th Int. Conf. on Hadron Spectroscopy, Beijing, China, Aug. 24–28, 1999*, Nucl. Phys. A **675**, 209 (2000).
6. S. Narison, *Proc. 8th Int. Conf. on Hadron Spectroscopy, Beijing, China, Aug. 24–28, 1999*, Nucl. Phys. A **675**, 54 (2000); Nucl. Phys. Proc. Suppl. **86**, 242 (2000).
7. F.E. Close, A. Kirk, Phys. Lett. B **483**, 345 (2000).
8. N.A. Törnqvist, Phys. Rev. Lett. **49**, 624 (1982).

9. S.V. Bashinsky and B.O. Kerbikov, Phys. Atom. Nucl. **59**, 1979 (1996).
10. C. Caso et al. (Particle Data Group), Eur. Phys. J. C **3**, 1 (1998).
11. S. Teige et al., Phys. Rev. D **59**, 012001 (1998).
12. L. de Billy et al., Nucl. Phys. B **176**, 1 (1980).
13. A. Abele et al., Phys. Rev. D **57**, 3860 (1998).
14. C. Amsler et al., Phys. Lett. B **333**, 277 (1994).
15. D. Barberis et al. (WA102 Collaboration), Phys. Lett. B **440**, 225 (1998).
16. V. Chernyshev et al., COSY proposal #55 "Study of a_0^+ mesons at ANKE" (1997) and M. Büscher et al., beam-time request for COSY proposal #55; *available via www*: http://ikpd15.ikp.kfa-juelich.de: 8085/doc/Anke.html; L.A. Kondratyuk et al., Preprint ITEP 18-97, Moscow (1997).
17. V. Yu. Grishina et al. nucl-th/9905049; Phys. Lett. B **475**, 9 (2000).
18. V. Yu. Grishina et al., nucl-th/9906064; Yad. Fiz. **63** (2000).
19. S. Flatté, Phys. Lett. B **63**, 224 (1976).
20. D.V. Bugg, Phys. Rev. D **50**, 4412 (1994).
21. R. Machleidt, K. Holinde, and Ch. Elster, Phys. Rep. **149**, 1 (1987).
22. V. Mull and K. Holinde, Phys. Rev. C **51**, 2360 (1995).
23. M. Kirchbach, D.O. Riska, Nucl. Phys. A **594**, 419 (1995).
24. T. Feuster and U. Mosel, Phys. Rev. C **58**, 457 (1998); C **59**, 460 (1999).
25. M. Atkinson et al., Phys. Lett. B **138**, 459 (1984).
26. M.A. Abolins et al., Phys. Rev. Lett. **25**, 469 (1970).
27. A.A. Sibirtsev, Nucl. Phys. A **604**, 455 (1996).
28. D.L. Cheshire et al., Phys. Rev. Lett. **28**, 520 (1972).
29. N.N. Achasov and G.N. Shestakov, Phys. Rev. D **56**, 212 (1997); hep-ph/9710537.
30. A.B. Kaidalov, Sov. J. Nucl. Phys. **53**, 872 (1991).
31. L.A. Kondratyuk et al., Phys. Rev. C **48**, 2491 (1993).
32. D. Alde et al., Yad. Fiz. **41**, 126 (1985); D. Alde et al., Phys. Lett. B **205**, 397 (1988).
33. D. Alde et al., Phys. Atom. Nucl. **59**, 982 (1996); S. Sadovsky, *Proc. of the 6th Int. Conf. on Hadron Spectroscopy, Hadron'95*, edited by M.C. Birse et al., (World Scientific Publ. Co., 1996) p. 445.
34. A.R. Dzierba, in *Proceedings of the Second Workshop on Physics and Detectors for DAΦNE'95, Frascati, 1995*, edited by R. Baldini et al., Frascati Physics Series **4**, 99 (1996).
35. R. Kokoski and N. Isgur, Phys. Rev. D **35**, 907 (1987).
36. A.B. Kaidalov, in Surveys High Energy Phys., **13**, 265 (1999).
37. M. Lacombe et al., Phys. Lett. B **101**, 139 (1981).